# PREPARATION AND MAGNETIC CHARACTERIZATION OF ($Fe_{78}B_{14}Si_8$)-NB-Y BULK METALLIC GLASS

**R. Piccin, P. Tiberto, M. Baricco, N. Lecis, M.Vedani**

*In the present work, the glass formation of $Fe_{78}B_{14}Si_8$ alloy with small additions of Nb and Y has been investigated. Ribbons were prepared by planar-flow casting. Small ingots (up to 5 mm in diameter) were obtained by injection casting technique into a cylindrical Cu mold. Thermal and structural properties were measured using differential scanning calorimetry (DSC) and X-Ray diffraction (XRD), respectively. The microstructure has been observed by Scanning Electron Microscopy (SEM). Quasi-static hysteresis loops have been measured using a vibrating sample magnetometer (VSM). Rapid solidification leads to a fully amorphous structure for all compositions. A fully amorphous structure has been obtained in samples prepared by copper mold casting, when adding Nb and Y. The role of Nb and Y addition on glass formation is discussed on the basis of melting behavior, analyzed by HT-DSC. Magnetic properties are correlated with the observed microstructures.*

KEYWORDS: amorphous alloys, solidification, diffractometry, metallography, magnetic properties

## INTRODUCTION

Bulk metallic glasses (BMG) have been extensively studied due to their potential technological applications and their interesting physical properties such as a low modulus of elasticity, high yielding stress and good magnetic properties [1]. In the particular case of the magnetic properties, the Nd-Fe-Al-based BMG presents good hard magnetic properties: very high coercive fields and high energy product values [2]. In the other side, the Fe-based BMG presents good soft magnetic properties, with low coercive fields, high permeability values and low power losses. Amorphous Fe-Si-B alloys are used as transformer core materials due to their good soft magnetic properties. The glass forming ability of these materials has been studied experimentally in the past [3]. More specifically, the most favorable Fe–Si–B glasses concerning their thermal stability have 5–15 at.% Si and 75–78 at.% Fe [4] and indeed, the compositions of metallic glasses with the greatest technological significance are in this region [5]. However, the fully amorphous structure can be achieved below maximum thicknesses of 230 $\mu$m [3]. In order to improve the glass forming ability (GFA), the minor alloying addition is a very effective method [6]. It was reported that small additions of Nb and Y improve the GFA of Fe-based alloys and their role has been related to thermodynamic, kinetic and structural effects [7,8]. The addition of a large atom such as Y helps to destabilize the competing crystalline phases due to its large negative heat of mixing with other small and intermediate atoms [9]. Moreover, Y was found to be able to scavenge oxygen from the undercooled liquid avoiding the heterogeneous nucleation and increasing furthermore the GFA. Nb addition enables the formation of stable amorphous phase through an increase in the stability of the supercooled liquid against crystallization due to its negative heats of mixing compared to Fe, Si and B [1,9].

The aim of this paper is to investigate the role of addition of Nb and Y to a widely used magnetic amorphous alloy $Fe_{78}B_{14}Si_8$. The GFA has been analyzed comparing the results obtained by rapid solidification and by copper mold casting. It appears that the addition of both Nb and Y promotes bulk glass formation. The melting and solid-

**R. Piccin, M. Baricco**
Dipartimento di Chimica IFM e NIS, Università di Torino, Torino
**P. Tiberto**
Istituto Nazionale di Ricerca Metrologica, Torino
**N. Lecis, M.Vedani**
Dipartimento di Meccanica, Politecnico di Milano, Milano

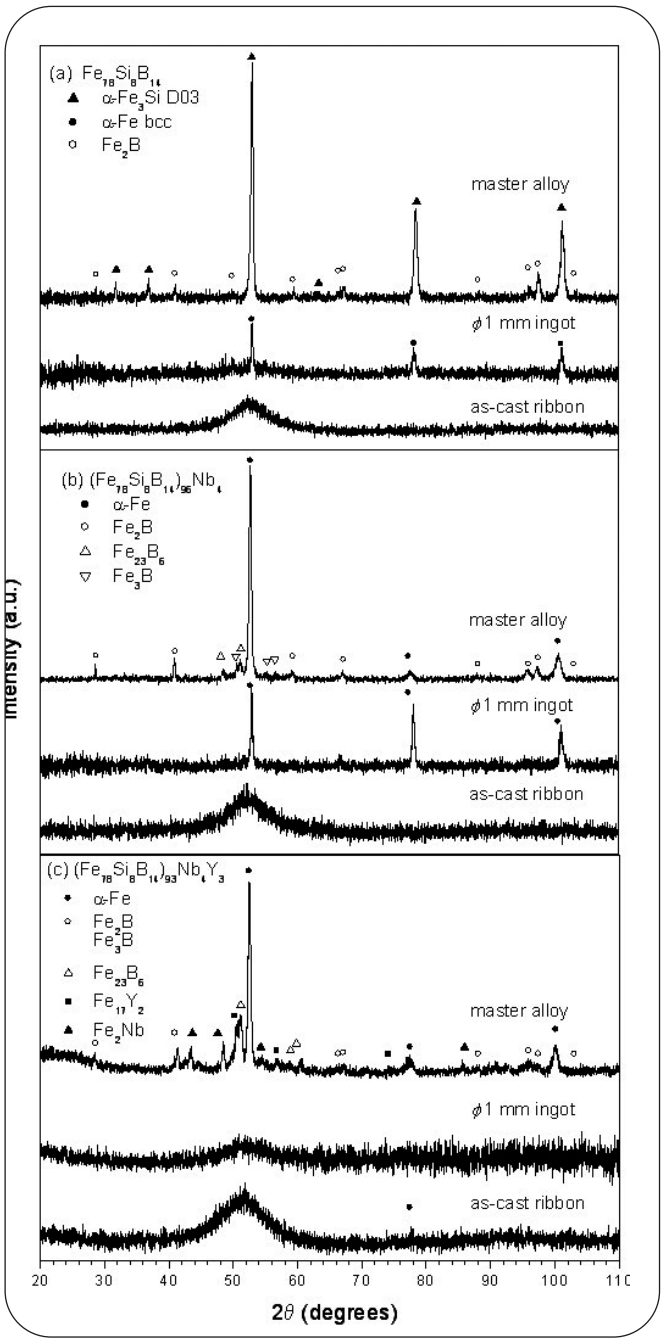


Fig. 1

***XRD patterns of master alloy, as-cast ingot and as-quenched ribbon: (a) $Fe_{78}B_{14}Si_8$, (b) $(Fe_{78}B_{14}Si_8)_{96}Nb_4$ and (c) $(Fe_{78}B_{14}Si_8)_{93}Nb_4Y_3$.***

*Diffratogrammi raggi X delle leghe madri, lingotti as-cast e nastri as-quenched di composizioni: (a) $Fe_{78}B_{14}Si_8$, (b) $(Fe_{78}B_{14}Si_8)_{96}Nb_4$ e (c) $(Fe_{78}B_{14}Si_8)_{93}Nb_4Y_3$.*

ification behavior of various alloys has been investigated by HT-DSC, showing a decrease of the melting temperature due to minor additions to the base alloy. From the SEM analysis of the microstructure of $(Fe_{78}Si_8B_{14})_{93}Nb_4Y_3$ master alloy, the presence of an immiscibility gap in the liquid state is inferred. The analysis of magnetic properties indicates a better behavior for the amorphous ribbon with respect to bulk metallic glass.

## EXPERIMENTAL

$Fe_{78}B_{14}Si_8$, $(Fe_{78}B_{14}Si_8)_{96}Nb_4$ and $(Fe_{78}B_{14}Si_8)_{93}Nb_4Y_3$ master alloys have been prepared by arc melting 99.9% pure elements in a Ti-gettered argon atmosphere. The alloys have been melted several times in order to improve their homogenization. Ribbons with thicknesses between 30 and 60 $\mu$m have been prepared by planar-flow casting in Ar atmosphere. The master alloy was melted in a quartz crucible (with an open nozzle of 0.8 mm) using an induction coil and ejected thereafter in a cylindrical-shaped Cu mold by applying an overpressure of about 1.5 bar. The bulk cast alloys have been prepared as cylinders with 1 mm base and 30 mm height.

The structure of the samples has been checked by X-ray diffraction (XRD) using Co-$K_\alpha$ radiation. Alloys melting and solidification processes have been studied by using a Setaram HT-DSC at scanning rate of 0.033 $Ks^{-1}$. The sample was introduced in an alumina pan and surrounded with alumina powder to prevent sticking to the crucible walls. The cell was evacuated and purged several times before measuring, under He flow. Calibration of the instrument has been performed by measuring the temperature and heat of fusion of samples of pure metals (Al, Ag, Au, Fe, Cu, Ni). The evolution of the crystallization process of the amorphous samples has been studied by Perkin Elmer DSC7 using a heating rate of 0.33 $Ks^{-1}$ under Ar flow. Microstructure analysis has been carried out on samples previously etched with 2 % Nital using a Leika Stereoscan 420 Scanning Electron Microscope (SEM). Samples composition and homogeneity were verified by energy dispersive spectroscopy (EDS).

DC-magnetic measurements were carried out using a vibration sample magnetometer (VSM) and a home made loop tracer. The applied magnetic field was parallel to the casting direction of the samples. In the case of ribbons, the analyzed pieces with dimension of 3.0 x 3.0 $mm^2$ were cut from a master ribbon. The measured cylindrical ingots had 1.0 mm diameter and around 20 mm height.

## RESULTS AND DISCUSSION

XRD patterns of the ternary $Fe_{78}B_{14}Si_8$ alloy, referred as base alloy hereafter, are shown in Fig. 1-(a). The presence of the ordered $Fe_3Si$ (D03) and $Fe_2B$ phases is observed in the master alloy. In the rapidly solidified ribbons the formation of such phases was suppressed and the presence of a main halo indicates a fully glassy phase. In the ingot case, only bcc-Fe peaks are observed in the XRD pattern. Fig. 1-(b) shows the XRD patterns of the $(Fe_{78}B_{14}Si_8)_{96}Nb_4$ alloy. Bcc-Fe and a mixture of borides ($Fe_2B$, $Fe_3B$, $Fe_{23}B_6$) are observed in the master alloy. No Nb-containing phases were observed, suggesting the dissolution of this element in the equilibrium phases. The formation of borides was suppressed in the as-cast ingot and only diffraction peaks of bcc-Fe can be observed. Rapid solidification leads to a fully amorphous phase, as evidenced by the absence of diffraction peaks in the XRD pattern. Fig. 1-(c) shows the XRD patterns of the $(Fe_{78}B_{14}Si_8)_{93}Nb_4Y_3$ alloy. Diffraction peaks corresponding to bcc-Fe, borides mixture ($Fe_2B$, $Fe_3B$, $Fe_{23}B_6$), $Fe_{17}Y_2$ and $Fe_2Nb$ phases were identified in the master alloy pattern. In the case of the as-cast ingot, only a main halo was observed, confirming the presence of fully amorphous phase. The as-

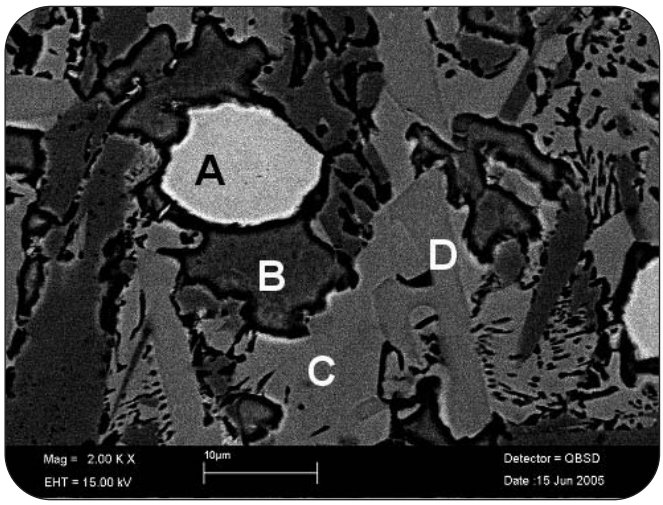


Fig. 2

***Back-scattered SEM images of $(Fe_{78}B_{14}Si_8)_{96}Nb_4Y_3$ master alloy containing $Fe_2Nb$ phase (A), bcc-Fe (B), boride phases (C) and $Fe_{17}Y_2$ phase (D).***

*Immagine SEM a elettroni retrodiffusi della lega madre $(Fe_{78}B_{14}Si_8)_{93}Nb_4Y_3$. Fasi identificate: (A) $Fe_2Nb$, (B) Fe-bcc, (C) boruri e (D) $Fe_{17}Y_2$.*

cast ribbon pattern also presents only a main halo corresponding to the amorphous phase. A weak (200) diffraction peak of bcc-Fe is also observed in the pattern, indicating the presence of a small fraction of oriented crystals on the surface.

Fig. 2 shows the back-scattered SEM images of the microstructure of the $(Fe_{78}B_{14}Si_8)_{93}Nb_4Y_3$ master alloy. The image of the master alloy indicates a heterogeneous microstructure spread over the whole sample and the presence of four equilibrium phases is clearly evidenced from the observed contrast. Equilibrium phases in the master alloy were identified from the chemical composition data measured in several areas of the sample. The brighter phase was identified as being $Fe_2Nb$ (A), and concerning its drop-like shape, it is believed that this phase had solidified from a Nb-enriched liquid that has been separated from the parent liquid. Such liquid separation occurs due to presence of miscibility gap of the binary Nb-Y system that can be extended to more complex systems [10]. (B) and (C) areas in Fig. 2 were identified as bcc-Fe and boride phases, respectively, which were formed from a pseudo-eutectic reaction. A coarse $Fe_{17}Y_2$ microstructure (D) was also identified and it is expected to be formed from a solid-state reaction at low temperature. SEM image of the cross section of the as cast ingot and ribbon (not shown here) did not show any significant contrast, confirming the formation of a fully amorphous phase by rapid solidification.

In order to understand the effect of Nb and Y addition on glass formation, the melting behavior of $Fe_{78}B_{14}Si_8$, $(Fe_{78}B_{14}Si_8)_{96}Nb_4$ and $(Fe_{78}B_{14}Si_8)_{93}Nb_4Y_3$ alloys has been investigated by HT-DSC. Melting and solidification curves are shown in Fig. 3 and the relevant thermal stability properties are collected in Table I. The ternary base alloy (Fig. 3-(a)) exhibits three endothermic peaks. According to the assessed Fe-Si-B phase diagram [11], the first peak ($T_M$) can be associated to the first melting reac-

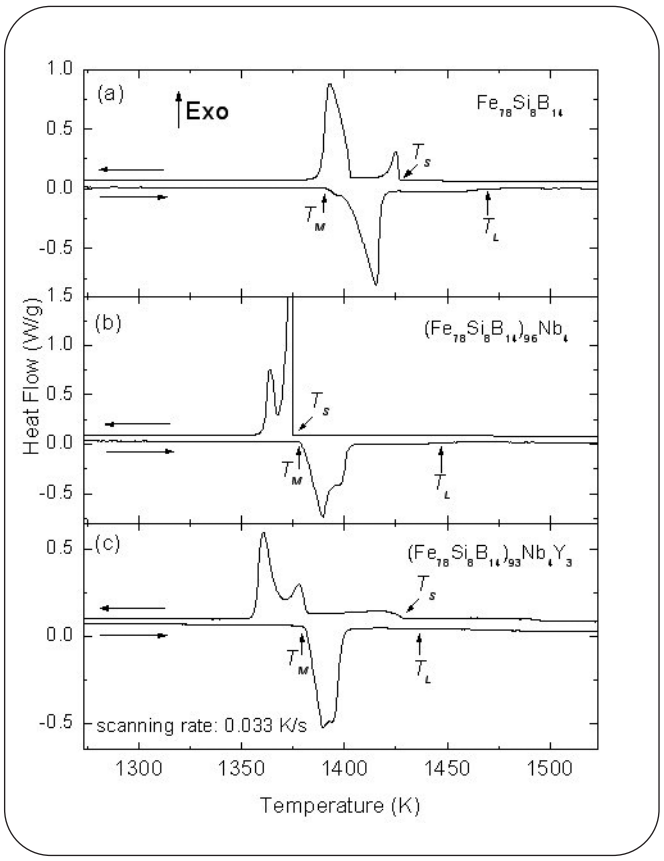


Fig. 3

***High temperature DSC for (a) $Fe_{78}B_{14}Si_8$, (b) $(Fe_{78}B_{14}Si_8)_{96}Nb_4$ and (c) $(Fe_{78}B_{14}Si_8)_{93}Nb_4Y_3$ alloys. Arrows indicate TM, TR and TL reported in Tab. 1.***

*Tracce DSC ad alta temperatura delle leghe (a) $Fe_{78}B_{14}Si_8$, (b) $(Fe_{78}B_{14}Si_8)_{96}Nb_4$ e (c) $(Fe_{78}B_{14}Si_8)_{93}Nb_4Y_3$. Le frecce indicano TM, TR and TL riportate nella Tab. 1.*

tion of the bcc-Fe/$Fe_2B$ mixture. The main reaction corresponds to the melting of $Fe_2B$ and it is followed by the liquidus point ($T_L$) at higher temperatures, where the bcc-Fe is fully transformed into the liquid. Solidification of the liquid alloy shows a slight undercooling, as evidenced by the huge exothermic signal due to primary solidification. Two solidification reactions, partially overlapped, follow without any significant undercooling. The DSC curve for the $(Fe_{78}B_{14}Si_8)_{96}Nb_4$ alloy, shown in Fig. 3-(b), displays that the first melting reaction, occurring at 1378 K, is followed by an overlapped endothermic peak. Liquidus point was measured at 1448 K. Solidification of this alloy shows a strong liquid undercooling, as already observed for similar compositions [7]. For the $(Fe_{78}B_{14}Si_8)_{93}Nb_4Y_3$ alloy the two melting reactions start at 1381 K and appear almost fully overlapped, as shown in Fig. 3-(c). The liquidus point is barely visible on heating at 1436 K, but it is clearly observable, after a small undercooling, on the HT-DSC trace of solidification. From the whole data of HT-DSC, it is clear that the addition of Nb reduces both $T_M$ and $T_L$ of the $Fe_{78}B_{14}Si_8$ alloy. The successive addition of Y to $(Fe_{78}B_{14}Si_8)_{96}Nb_4$ does not influence significantly $T_M$ and $T_L$ values.

Fig. 4 shows DSC traces obtained for rapidly solidified ribbons. The glass transition temperature cannot be evi-

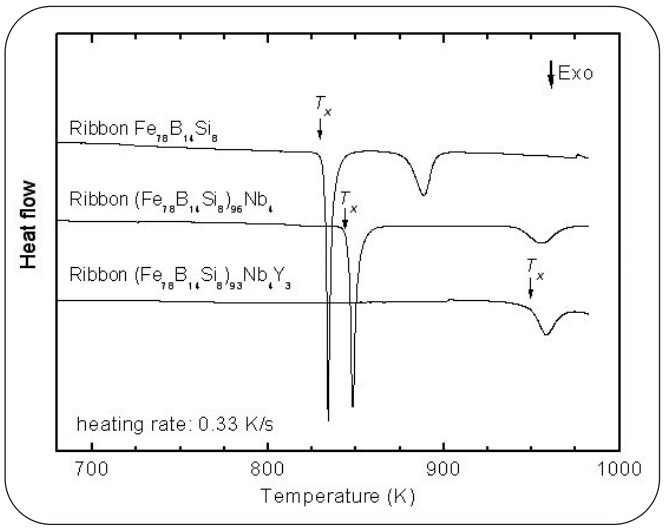


Fig. 4

***DSC traces of crystallization for as-quenched amorphous ribbons.***
*Tracce DSC della cristallizzazione di nastri amorfi as-quenched.*

| Alloy composition | $T_x$ (K) | $T_M$ (K) | $T_L$ (K) | $T_S$ (K) |
|---|---|---|---|---|
| $Fe_{78}B_{14}Si_8$ | 830 | 1392 | 1468 | 1427 |
| $(Fe_{78}B_{14}Si_8)_{96}Nb_4$ | 844 | 1378 | 1448 | 1375 |
| $(Fe_{78}B_{14}Si_8)_{93}Nb_4Y_3$ | 948 | 1381 | 1436 | 1428 |

Tab. 1

***Thermal stability properties obtained from DSC traces. $T_M$ - melting temperature, $T_L$ - liquidus, $T_S$ - solidification temperature and $T_x$ - crystallization temperature of amorphous ribbons.***
*Proprietà termiche ottenute dalle tracce di DSC. $T_M$ - temperatura di fusione, $T_L$ - temperatura di liquidus, $T^S$ - temperatura di solidificazione e $T_x$ - temperatura di cristallizzazione.*

denced. The crystallization temperature ($T_x$) is marked by arrows on the DSC traces and the corresponding values are reported in Tab. 1. $Fe_{78}B_{14}Si_8$ and $(Fe_{78}B_{14}Si_8)_{96}Nb_4$ alloys exhibit two resolved exothermal reactions. The first peak corresponds to the formation of α-Fe phase and the second one to the formation of $Fe_2B$ phase [12]. Single exothermic peaks due to the crystallization of the glassy phase were found for $(Fe_{78}B_{14}Si_8)_{93}Nb_4Y_3$ amorphous alloy in the temperature range accessible by the DSC7. The Nb addition to the base alloy increases $T_x$ from 830 K to 844 K and a further addition of Y increases $T_x$ to 948 K.
The magnetization curves of the as-cast ingots and as-quenched amorphous ribbons are shown in Fig. 5 for: $Fe_{78}B_{14}Si_8$, $(Fe_{78}B_{14}Si_8)_{96}Nb_4$ and $(Fe_{78}B_{14}Si_8)_{93}Nb_4Y_3$ alloys. The measurements were performed with a maximum applied field of 25 kA/m. The saturation magnetization ($M_S$) and coercive field ($H_C$) values for ribbons and as-cast ingots are presented in Tab. 2. In the case of as-cast ingots (Fig. 5-(a)), quite high coercive fields were measured for $Fe_{78}B_{14}Si_8$ and $(Fe_{78}B_{14}Si_8)_{96}Nb_4$ alloys, indicating the presence of crystalline grains that hinder the movement of the magnetic domain

| Alloy composition | Ribbon | CM Ingot (0.8 mm) |
|---|---|---|
| | $M_S$ (μ$_0$T) | |
| $Fe_{78}B_{14}Si_8$ | 1.27 | 0.31* |
| $(Fe_{78}B_{14}Si_8)_{96}Nb_4$ | 1.16 | 1.12 * |
| $(Fe_{78}B_{14}Si_8)_{93}Nb_4Y_3$ | 0.91 | 0.91 |
| | $H_C$ (A/m) | |
| $Fe_{78}B_{14}Si_8$ | 90 | 9820 |
| $(Fe_{78}B_{14}Si_8)_{96}Nb_4$ | 40 | 4280 |
| $(Fe_{78}B_{14}Si_8)_{93}Nb_4Y_3$ | 55 | 170 |

Tab. 2

***Magnetic properties of $Fe_{78}Si_8B_{14}$, $(Fe_{78}Si_8B_{14})_{96}Nb_4$ and $(Fe_{78}Si_8B_{14})_{93}Nb_4Y_3$ alloys. $M_S$ - saturation magnetization and $H_C$ - coercive field. *Non saturated values.***
*Proprietà magnetiche delle leghe $Fe_{78}Si_8B_{14}$, $(Fe_{78}Si_8B_{14})_{96}Nb_4$ e $(Fe_{78}Si_8B_{14})_{93}Nb_4Y_3$. $M_S$ - magnetizzazione di saturazione e $H_C$ - campo coercitivo. *Valori non saturati.*

walls. In both measurements, the maximum applied field was not enough to saturate these samples. The hysteresis loop of $(Fe_{78}B_{14}Si_8)_{93}Nb_4Y_3$ as-cast ingot has a smaller $H_C$ value (170 A/m), associated with a complete amorphous phase. In the case of the amorphous ribbons (Fig. 5-(b)), the addition of Nb and Y decreases $M_S$ values. Such a decrease can be explained by the presence of non-magnetic atoms inside the glassy phase, which changes the magnetic response of the matrix. Typical magnetically soft $H_C$ values were obtained for ribbons of all compositions and slight decreases were observed when Nb and Y are added. It is worth to mention that the magnetic measurements are in agreement with XRD results and one can associate the presence of a main amorphous halo with low $H_C$ values for this kind of alloy.

## CONCLUSIONS

The effect of small additions of Nb and Y on glass formation of the ternary $Fe_{78}B_{14}Si_8$ alloy has been examined. Fully amorphous ribbons were obtained by rapid solidification. Amorphous 1 mm ingots were obtained by adding 4 at % Nb and 3 at.% Y, as confirmed by XRD and DSC measurements. The high temperature DSC analysis showed that the addition of Nb and Y lowers the melting temperature and increases the undercooled liquid region of the alloys.
The magnetic measurements indicate a soft magnetic behavior for the as-cast ribbons. The saturation magnetization of the as-cast ribbons decreases with the addition of Nb and Y due to the presence of non-magnetic atoms inside the amorphous phase. The as-cast ingot $(Fe_{78}B_{14}Si_8)_{93}Nb_4Y_3$ has also good soft magnetic properties due to the presence of a complete amorphous phase, while $Fe_{78}B_{14}Si_8$ and $(Fe_{78}B_{14}Si_8)_{96}Nb_4$ as-cast ingots presented poor soft properties due to the presence of a high crystalline fraction.

## ACKNOWLEDGMENTS

Work performed for COFIN/MIUR 2005097983_002 and for MRTN-CT-2003-504692. RP is supported by the

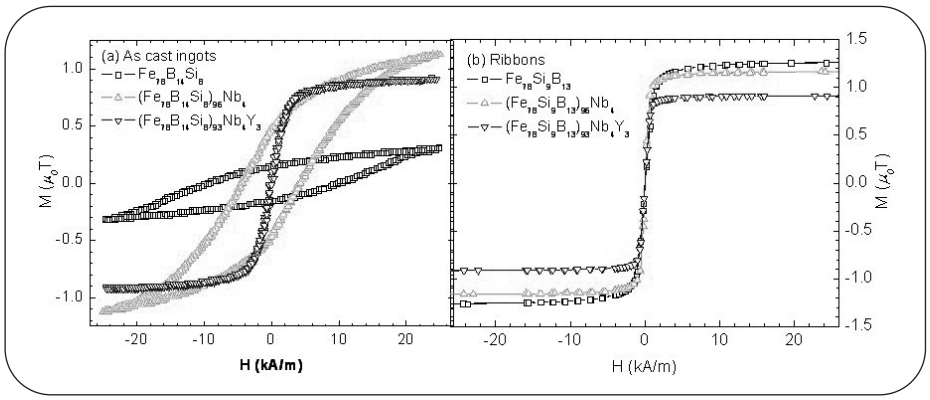


Fig. 5 ***Magnetization curves for: (a) as-cast ingots and (b) as-quenched amorphous ribbons.***
*Curve di magnetizzazione di: (a) lingotti as-cast e (b) nastri amorfi as-quenched.*

Programme Al,an, the European Union Programme of High Level Scholarships for Latin America, scholarship no. E04D036521BR. H. Chiriac and N. Lupu in the frame of Italy / Romania Scientific Program (project number 13).

## REFERENCES

[1] N. NISHIYAMA, K. AMIYA, A. INOUE, Mater. Trans. 45 (2004) 1245.
[2] R.W. McCALLUM, L.H. LEWIS, M.J. KRAMER, K.W. DENNIS, J. Magn Magn Mat 299 (2006) 265.
[3] M. MITERA, M. NAKA, T. MASUMOTO, N. KAZAMA, H. WATANABE, Phys. Status. Sol. (a) 49 (1978) 163.
[4] K. CHRISSAFIS, M.I. MARAGAKIS, K.G. EFTHIMIADIS, E.K. POLYCHRONIADIS, J. All. Comp. 386 (2005) 165.
[5] I. MATKO, E. ILLEKOVA, P. SVEC, P. DUHAJ, Mater. Sci. Eng. A 225 (1997) 145.
[6] Z.P. LU, C.T. LIU, J. Mater. Sci. 39 (2004) 3965.
[7] A. INOUE, B. SHEN, Mater. Trans. 43 (2002) 766.
[8] D.S. SONG, J.-H. KIM, E. FLEURY, W.T. KIM and D.H. KIM, J. All. Comp. 389 (2005) 159.
[9] F.R. de BOER, R. BOOM, W. C. M. MATTERNS, A.R. MIEDEMA, A. K. NIESSEN, "Cohesion in Metals", (North-Holland, Amsterdam, 1988)
[10] N. MATTERN, U. KUHN, A. GEBET, T. GEMMING, M. ZINKEVICH, H. WENDROCK, L. SCHULTZ, Scripta Mater. 53 (2005) 271-274.
[11] T. TOKUNAGA, H. OHTANI, M. HASEBE, Comp. Coupling of Phase Diagram and Thermochemistry 28 (2004) 354.
[12] D.S. dos SANTOS, D.R. dos SANTOS, J. Non-Cryst. Sol. 304 (2002) 56.

# ABSTRACT

### PREPARAZIONE E CARATTERIZZAZIONE MAGNETICA DI LEGHE AMORFE MASSIVE ($Fe_{78}B_{14}Si_8$)-NB-Y

*Parole chiave: leghe amorfe, solidificazione, diffrattometria, metallografia, proprietà magnetiche*

*Fasi amorfe sono state sintetizzate già da alcuni decenni anche nel caso di materiali metallici grazie all'utilizzo di tecniche di rapida solidificazione, che consistono nell'eiezione della lega liquida su di una ruota metallica in rapida rotazione, in modo da produrre nastri continui, tipicamente dello spessore di 10-50 micrometri. Solo in anni recenti, le peculiari proprietà delle leghe amorfe hanno guidato la ricerca verso la sintesi di vetri metallici massivi (lingotti di alcuni millimetri di spessore). Questi si ottengono attraverso accurate tecniche di solidificazione e solo per alcune leghe di particolare composizione, caratterizzate da una tendenza particolarmente spiccata a formare fasi amorfe. Proprietà magnetiche dolci sono state messe in evidenza in leghe amorfe massive a base Fe, mentre proprietà come materiali magnetici duri sono state osservate nel sistema Nd-Fe-Al.*
*In questo lavoro verranno presentati i risultati della sintesi e caratterizzazione magnetica di vetri metallici massivi nel sistema ($Fe_{78}B_{14}Si_8$)-Nb-Y. Infatti, per promuovere formazione di una fase vetrosa nella lega $Fe_{78}B_{14}Si_8$ è stato osservato che risultano particolarmente vantaggiose aggiunte di piccole quantità di Nb e Y. Nastri amorfi sono stati prodotti tramite tecniche di rapida solidificazione (planar-flow casting) mentre la preparazione di lingotti cilindrici con diametro 1 mm e lunghezza 30 mm è stata condotta per mezzo di colata in stampo di rame. Le fasi presenti nei campioni sono state individuate mediante diffrazione di raggi X e la loro microstruttura è stata osservata tramite microscopia elettronica a scansione (SEM). Le analisi termiche della cristallizzazione e della fusione sono state effettuate tramite calorimetria differenziale a scansione (DSC). La caratterizzazione magnetica è stata condotta mediante un magnetometro VSM e con tecniche induttive.*
*Mediante fusione in forno ad arco sono state preparate leghe madri di composizione: ($Fe_{78}B_{14}Si_8$), ($Fe_{78}B_{14}Si_8$)$Nb_4$, ($Fe_{78}B_{14}Si_8$)$Nb_4Y_3$. La rapida solidificazione ha prodotto nastri amorfi per tutte le leghe. Solo la composizione quinaria ($Fe_{78}B_{13}Si_9$)$Nb_4Y_3$ ha prodotto una lega completamente amorfa (con un diametro massimo di 1 mm), mentre per le altre composizioni sono state ottenute leghe parzialmente cristalline (Fig. 1). L'aggiunta di Nb ed Y al sistema $Fe_{78}B_{14}Si_8$ provoca una riduzione della temperatura di fusione, che passa da 1392 K a 1381 K (Fig. 3 e Tabella I). Le leghe amorfe cristallizzano nell'intervallo di temperatura compreso tra 830 K e 950 K (Fig. 4). Da un confronto tra le temperature di fusione e di cristallizzazione delle diverse leghe, determinate mediante l'analisi termica, è stato possibile giustificare la maggiore tendenza alla formazione di una fase vetrosa da parte del sistema ($Fe_{78}B_{14}Si_8$)$Nb_4Y_3$. Le proprietà magnetiche (ie. coercitività, permeabilità magnetica e magnetizzazione di saturazione; Fig. 5 e Tab. 2) sono correlate alla microstruttura delle leghe. Infatti, la presenza di una fase cristallina tende ad incrementare significativamente la coercitività ed a ridurre la permeabilità magnetica. Nel caso dei campioni massivi completamente amorfi, sono state osservate buone proprietà magnetiche dolci, con un campo coercitivo inferiore a 200 A/m.*